



Conjugate observations of ENA signals in the high-altitude cusp and proton auroral spot in the low-altitude cusp with IMAGE spacecraft

S. Suzuki,¹ S. Taguchi,² K. Hosokawa,² M. R. Collier,³ T. E. Moore,³ H. U. Frey,⁴ and S. B. Mende⁴

Received 6 May 2008; accepted 15 May 2008; published 8 July 2008.

[1] On 28 April 2001, significant enhancements of neutral atom signals were detected in the direction of a high-altitude cusp by the Low-Energy Neutral Atom (LENA) imager onboard the Imager for Magnetopause-to-Aurora Global Exploration (IMAGE). Simultaneously, proton auroral emission was observed in the low-altitude cusp by the Far-Ultraviolet Instrument (FUV) on the IMAGE spacecraft. The temporal variations of their intensities showed a good correlation, suggesting they had a common source. During a brief period, the proton auroral spot moved antisunward and dawnward in conjunction with the motion of the ionospheric footprint of the LENA cusp signal. The Tsyganenko-96 model shows that the possible source location of the LENA cusp signals maps to the FUV spot. Considering the solar wind variations, we have attributed this “moving proton auroral spot” to a moving flux tube that was created by transient reconnection on the dayside magnetopause and contained relatively high proton densities. **Citation:** Suzuki, S., S. Taguchi, K. Hosokawa, M. R. Collier, T. E. Moore, H. U. Frey, and S. B. Mende (2008), Conjugate observations of ENA signals in the high-altitude cusp and proton auroral spot in the low-altitude cusp with IMAGE spacecraft, *Geophys. Res. Lett.*, *35*, L13103, doi:10.1029/2008GL034543.

1. Introduction

[2] The Low-Energy Neutral Atom (LENA) imager onboard the Imager for Magnetopause-to-Aurora Global Exploration (IMAGE) spacecraft is designed to image the two-dimensional distribution of energetic neutral atoms (ENAs) coming to the spacecraft from a 90° field-of-view (polar angle sector), swept through 360° every 2 min by spacecraft spin [Moore *et al.*, 2000]. LENA responds to the neutral atoms that have energies from 15 eV to at least 4 keV [Moore *et al.*, 2003], and detects the ENA emissions that are produced by the magnetosheath flow near the subsolar magnetopause through charge exchange with the Earth’s hydrogen exosphere [e.g., Collier *et al.*, 2001]. The LENA signals are also observed in the direction of the high-altitude cusp [Taguchi *et al.*, 2004, 2005; Murata *et*

al., 2007]. These signals represent ion injection along a newly reconnected field line [Taguchi *et al.*, 2005].

[3] On the other hand, the Spectrographic Imager (SI12) of the Far-Ultraviolet Instrument (FUV) [Mende *et al.*, 2000] onboard the IMAGE spacecraft monitors the low-altitude cusp, which is identified as a proton auroral spot in the Doppler-shifted Lyman alpha emission [Frey *et al.*, 2002]. This proton auroral emission is produced by charge exchange and deexcitation of precipitating protons. Recent studies with FUV data have clarified the characteristics of the cusp proton injection caused by reconnection on the magnetopause [e.g., Chang *et al.*, 2002; Frey *et al.*, 2002, 2003; Fuselier *et al.*, 2002; Phan *et al.*, 2003]. The location of the cusp proton auroral spot can be largely accounted for by the anti-parallel reconnection site, and hence the interplanetary magnetic field (IMF) orientation, although there are cases to which the IMF B_y dependence is not applicable [Bobra *et al.*, 2004]. The SI12 detector is mostly sensitive to the proton precipitation in the energy range of 2–8 keV [Gérard *et al.*, 2001], and this range overlaps the range in which LENA responds, which allows us to examine the high- and low-altitude cusps simultaneously. We report the results obtained from the conjugate observations of the ENA signals and proton auroral emission on 28 April 2001.

2. Observations

2.1. Correspondence Between LENA Signal and Proton Aurora

[4] During 0500–0630 UT on 28 April 2001, LENA measured ENA signals over a wide range of spin angle sector including the general cusp direction in the magnetosphere. Proton auroral emissions in the dayside ionosphere were also observed by FUV SI12 throughout this interval. Figure 1 shows the conception diagram of the conjugate observation with the IMAGE spacecraft. If the primary source of the LENA cusp signal is the proton injection, it is expected that the LENA signal in the high-altitude cusp and the FUV emission in the low-altitude cusp have correlative variations.

[5] Figure 2 shows the LENA hydrogen total count in the cusp direction (Panel d), which is defined as a spin angle in the range of 157°–221° [Murata *et al.*, 2007], and the FUV emission in the cusp ionosphere (Panel e) for the 0500–0630 UT interval together with ACE solar wind observations (Panels a–c). For the FUV emission, the value averaged over the area of magnetic latitude (MLAT) of 70°–80° and magnetic local time (MLT) of 1000–1300 is plotted. The MLT range is set asymmetrically in order to avoid contamination of main oval emission, which will be

¹Sugadaira Space Radio Observatory, University of Electro-Communications, Tokyo, Japan.

²Department of Information and Communication Engineering, University of Electro-Communications, Tokyo, Japan.

³NASA Goddard Space Flight Center, Greenbelt, Maryland, USA.

⁴Space Science Laboratory, University of California, Berkeley, California, USA.

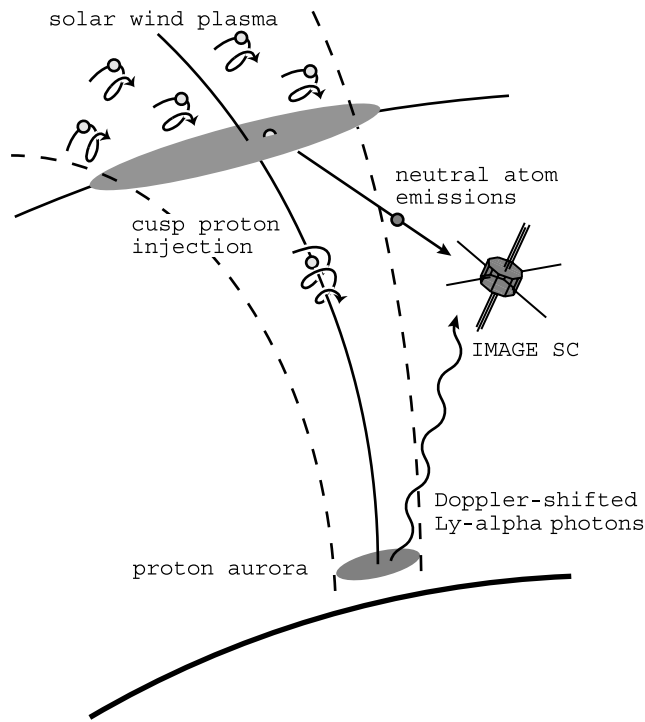


Figure 1. Schematic diagram of the conjugate observation of ENAs coming from the high-altitude cusp and proton auroral emissions in the low-altitude cusp with the IMAGE spacecraft. During an event presented in this paper IMAGE was located at $(X_{GSM}, Z_{GSM}) \sim (4.0\text{--}4.2 \text{ Re}, 3.3\text{--}6.0 \text{ Re})$ in the mid-noon sector ($Y_{GSM} \sim -1.0 \text{ Re}$).

shown later. We estimated the time lag from the ACE observation to the IMAGE FUV emission to be 28 min by relating the FUV emission enhancement at 0513 UT to the enhancement of the solar wind dynamic pressure at 0445 UT. Considering the possible time lag (2 min) from LENA signals to FUV emissions, the LENA signals are shifted by 2 min. The onset of the LENA cusp signal, which is observed at 0503 UT in Panel d, coincides with the start of a sudden impulse in the ground magnetic field, as has been shown by *Taguchi et al.* [2004].

[6] The IMF B_y and B_z components were positive except for a few short intervals. The solar wind dynamic pressure was relatively high throughout the interval. The variations of the solar wind dynamic pressure come from those of the solar wind density because the solar wind speed was relatively constant at $\sim 750 \text{ km s}^{-1}$ (not shown). The maximum density during this interval was 17 cm^{-3} , which will be discussed later. The variations of FUV intensities are correlated with those of the solar wind density or dynamic pressure, and the LENA signal also shows a correlative manner. These results indicate that both emissions are from a common source associated with the solar wind pressure.

2.2. Moving Proton Auroral Spot

[7] The top panels in Figure 3 are consecutive snapshots of the FUV emission obtained at ~ 0513 , ~ 0515 , and ~ 0517 UT, which correspond to the times A, B, and C in Figure 2, respectively. During this enhanced dynamic pressure period, a moving proton auroral spot with bright

FUV emission was identified. At time A, the spot appeared near local noon (peak; ~ 12.5 MLT and $\sim 73^\circ$ MLAT), and moved antisunward and dawnward until 0517 UT; then, it disappeared. The latitude of the spot is low considering that IMF B_z is positive. Note that the spot is located on the prenoon side at time C when IMF is $B_z \gg 0$ and $B_y > 0$. This is seemingly contradictory to the anti-parallel reconnection hypothesis [*Crooker, 1979*]. This will be discussed later.

[8] Figure 3 (bottom) show the ionospheric footprints of LENA images on the FUV contours. We mapped the LENA cusp signals to the geocentric sphere with a radius of 7.5 Re [*Taguchi et al., 2005*] and then traced the LENA images down to the ionospheric height of 110 km with the Tsyganenko 96 magnetic field line model [*Tsyganenko and Stern, 1996*]. The footprints of the LENA signals moved poleward and downward in a similar way to the FUV spot motion, although the downward motion of the LENA signal is somewhat unclear. Note that the LENA's field-of-view (FOV) is projected into the ionosphere at about 11–12 MLT and $72^\circ\text{--}77^\circ$ MLAT, which would miss the peak of the FUV spot at time A.

[9] We also investigated how the direction of the LENA cusp signal is aligned with magnetic field at $R = 7.5 \text{ Re}$. It is found that the direction of the line-of-sight for the LENA signal is almost parallel to the field line at $R = 7.5 \text{ Re}$, suggesting that the energetic neutrals detected by LENA in this study are created mostly by the ion injection along the field line.

3. Discussion and Conclusions

[10] From an FUV/LENA conjunction event on 28 April 2001, we have shown that the ENA signals in the high-altitude cusp and the proton auroral emission in the cusp ionosphere are well correlated in response to the solar wind variations. Such a remarkable correspondence of both emissions strongly suggests that the protons injected into the high-altitude cusp emit ENAs there and then produce the proton auroral spot in the low-altitude cusp, while precipitating into the ionosphere.

[11] Figure 4 shows a schematic summary of the moving proton auroral spot. At ~ 0513 UT, the bright proton auroral spot appeared in concurrence with the enhancements of the solar wind dynamic pressure and then moved antisunward and dawnward. The speed of the moving spot was estimated to be $\sim 2.4 \text{ km s}^{-1}$ from the FUV snapshots in Figure 3, which is a typical speed of the ionospheric convection for large IMF conditions like this event [e.g., *Maynard et al., 1991*]. *Maynard et al.* [1991] observed that large equatorward electric field $\sim 100 \text{ mV m}^{-1}$, equivalent to $\sim 2 \text{ km s}^{-1}$ of convection speed, in the southern low-altitude cusp for IMF $B_y \gg 0$ condition.

[12] Several studies on the dayside proton spot under northward IMF have revealed that the spot appears at latitudes poleward of the dayside oval ($\sim 80^\circ$ MLAT or more) in the prenoon or postnoon sector for IMF $B_y < 0$ or $B_y > 0$, respectively [e.g., *Frey et al., 2002*]. These responses of the cusp spot have been interpreted to be due to the changes in the reconnection point tailward of the high-altitude cusp. The moving proton auroral spot presented in this paper does not agree with such B_y dependence, that is, the spot was in the prenoon sector and at a relatively low

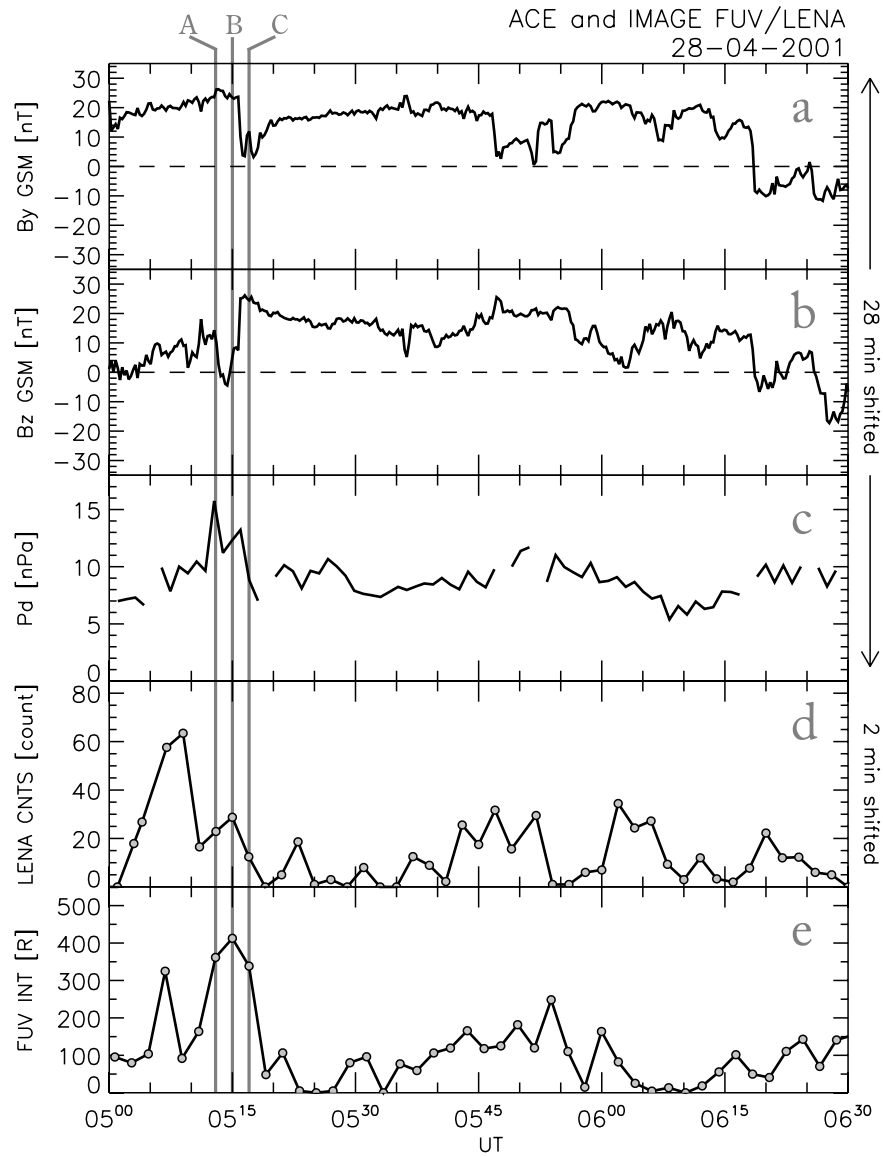


Figure 2. GSM components of IMF (a) B_y and (b) B_z , (c) solar wind dynamic pressure, (d) LENA hydrogen total count in the high-altitude cusp direction, and (e) FUV averaged emission in the cusp ionosphere for the event in this study. The ACE solar wind and LENA data are lagged by 28 and 2 min, respectively.

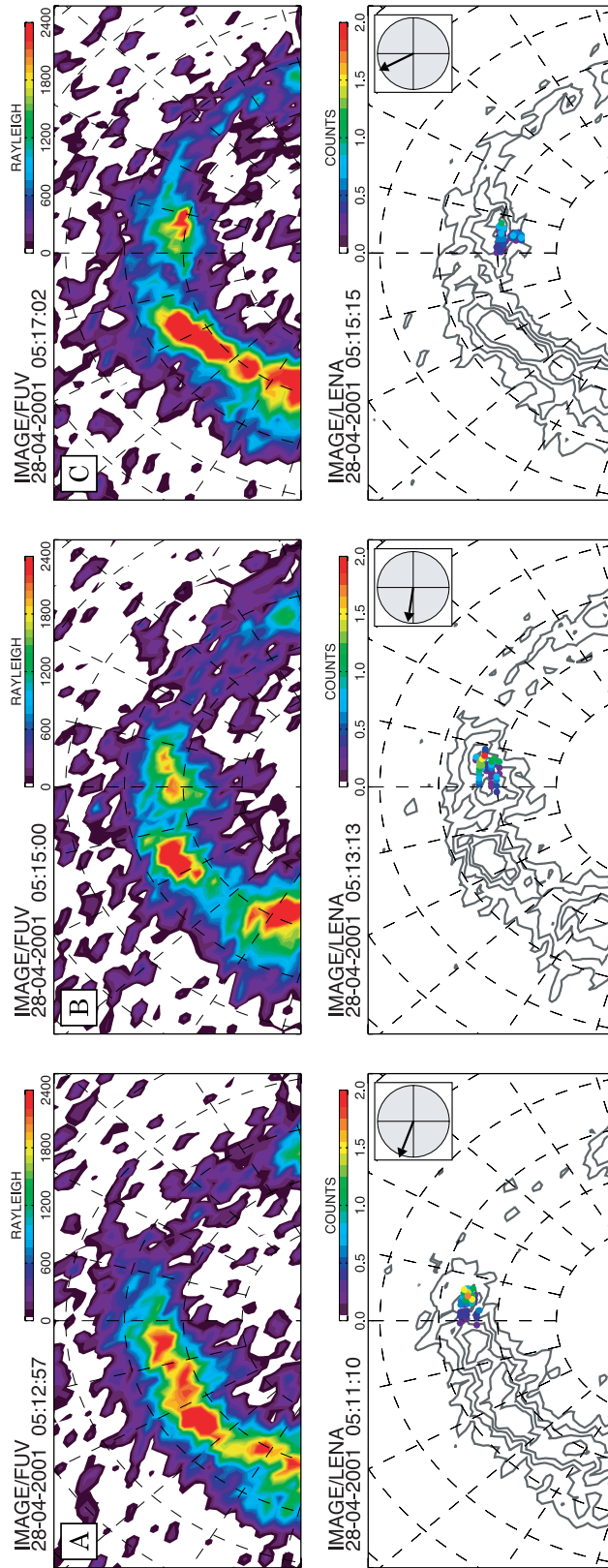


Figure 3. (top) Consecutive dayside proton aurora images obtained by FUV at the times of A, B, and C in Figure 2. The images are displayed in polar MLAT-MLT grid with 12 MLT towards the top of each panel, and dawn and dusk correspond to the bottom right and left, respectively. Dashed circles and lines are plotted every 5° (innermost: 80° MLAT) and 1 hour, respectively. (bottom) Ionospheric footprints of the LENA image overlotted on the FUV contours (gray lines). The IMF clock angles in GSM coordinates, shifted in time and sunward view, are shown in the upper right insets, with $B_z > 0$ pointing up and $B_y > 0$ pointing to the left.

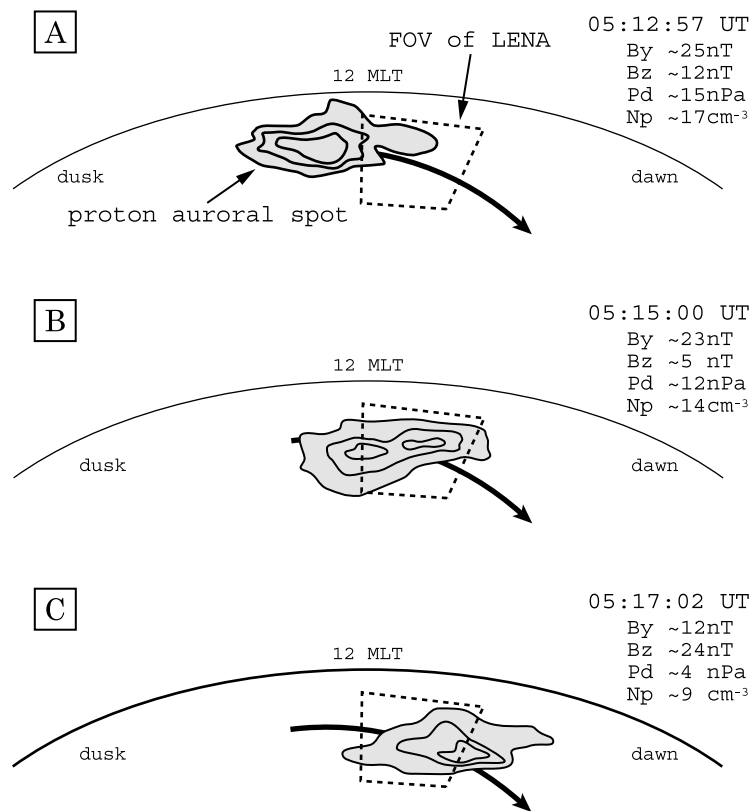


Figure 4. Schematic illustrations of the moving proton auroral spot at ~ 1513 , ~ 1515 , and ~ 1517 UT. Gray-colored contour represents the proton spot seen in the FUV image obtained at each time. Thick arrows and dashed squares indicate, respectively, the direction of the motion of the spot and the ionospheric projections of LENA's FOV for this interval. The solar wind conditions (B_y , B_z , dynamic pressure, and density) are shown in the upper right.

latitude (~ 73 – 75° MLAT), whereas the IMF B_y and B_z components were positive as shown in Figure 2.

[13] Recently, *Bobra et al.* [2004] have shown that the cusp spot locations for northward IMF cannot be accounted for only by the anti-parallel reconnection condition. The spots appeared either side of local noon for $B_y > 0$, although the anti-parallel reconnection site should be on the postnoon side. *Bobra et al.* [2004] have also proposed that the FUV emission in the unanticipated sector is due to the ion precipitation preferentially occurring in the prenoon magnetosphere, not associated with reconnection.

[14] Our interpretation for the moving proton auroral spot is as follows, and also provides an alternative explanation for the result by *Bobra et al.* [2004]: B_y -dominated IMF causes a dayside reconnection although the B_z component is positive. The IMF clock angle is larger than 60° at time A. The reconnected flux tube is “visualized” as an isolated auroral spot because it contains relatively high proton densities due to a brief period of high solar wind densities at the time of reconnection. Since IMF B_y is strongly positive, the flux tube moves downward with the convection flow. When this flux tube is away from noon (time C in Figure 4), IMF becomes $B_z \gg 0$ and $B_y > 0$. This suggests that the prenoon spot may be taken as a phenomenon for $B_z \gg 0$ and $B_y > 0$. In other words, the prenoon spots for $B_y > 0$ given by *Bobra et al.* [2004] may include a moving proton auroral spot, which is presented in this paper. At time C, cusp reconnection which is typical for strongly north-

ward IMF would occur on the postnoon side due to the positive B_y component. However, the proton auroral spot was not observed on the postnoon side in the ionosphere. This is reasonable because the solar wind dynamic pressure and density were no longer high.

[15] **Acknowledgments.** This work was supported by a grant-in-aid for Scientific Research of the Ministry of Education, Culture, Sports, Science and Technology of Japan (18540443) and by the IMAGE Project under UPN 370-28-20 at Goddard Space Flight Center. ACE solar wind data are provided by NASA/NSSDC.

References

- Bobra, M. G., S. M. Petrinec, S. A. Fuselier, E. S. Claflin, and H. E. Spence (2004), On the solar wind control of cusp aurora during northward IMF, *Geophys. Res. Lett.*, *31*, L04805, doi:10.1029/2003GL018417.
- Chang, S.-W., S. B. Mende, H. U. Frey, D. L. Gallagher, and R. P. Lepping (2002), Proton aurora dynamics in response to the IMF and solar wind variations, *Geophys. Res. Lett.*, *29*(13), 1648, doi:10.1029/2002GL015019.
- Collier, M. R., et al. (2001), Observations of neutral atoms from the solar wind, *J. Geophys. Res.*, *106*, 24,893–24,906.
- Crooker, N. U. (1979), Dayside merging and cusp geometry, *J. Geophys. Res.*, *84*, 951–959.
- Frey, H. U., S. B. Mende, T. J. Immel, S. A. Fuselier, E. S. Claflin, J.-C. Gérard, and B. Hubert (2002), Proton aurora in the cusp, *J. Geophys. Res.*, *107*(A7), 1091, doi:10.1029/2001JA900161.
- Frey, H. U., T. D. Phan, S. A. Fuselier, and S. B. Mende (2003), Continuous magnetic reconnection at Earth's magnetopause, *Nature*, *426*, 533–537.
- Fuselier, S. A., H. U. Frey, K. J. Trattner, S. B. Mende, and J. L. Burch (2002), Cusp auroral dependence on IMF B_z , *J. Geophys. Res.*, *107*(A7), 1111, doi:10.1029/2001JA900165.

- G erard, J.-C., et al. (2001), Observation of the proton aurora with IMAGE FUV imager and simultaneous ion flux in situ measurements, *J. Geophys. Res.*, *106*, 28,939–28,948.
- Maynard, N. C., T. L. Aggson, E. M. Basinska, W. J. Burke, P. Craven, W. K. Peterson, M. Sugiura, and D. R. Weimer (1991), Magnetospheric boundary dynamics: DE 1 and DE 2 observations near the magnetopause and cusp, *J. Geophys. Res.*, *96*, 3505–3522.
- Mende, S. B., et al. (2000), Far ultraviolet imaging from the IMAGE spacecraft: 3. Spectral imaging of Lyman- α and OI 135.6 nm, *Space Sci. Rev.*, *91*, 287–318.
- Moore, T. E., et al. (2000), The low-energy neutral atom imager for IMAGE, *Space Sci. Rev.*, *91*, 155–195.
- Moore, T. E., et al. (2003), Heliosphere-geosphere interactions using low energy neutral atom imaging, *Space Sci. Rev.*, *109*, 351–371.
- Murata, Y., S. Taguchi, K. Hosokawa, A. Nakao, M. R. Collier, T. E. Moore, N. Sato, H. Yamagishi, and A. S. Yukimatu (2007), Correlative variations of the neutral atom emission in the high-altitude cusp and the fast anti-sunward convection in the low-altitude cusp, *J. Geophys. Res.*, *112*, A11208, doi:10.1029/2007JA012404.
- Phan, T., et al. (2003), Simultaneous Cluster and IMAGE observations of cusp reconnection and auroral proton spot for northward IMF, *Geophys. Res. Lett.*, *30*(10), 1509, doi:10.1029/2003GL016885.
- Taguchi, S., M. R. Collier, T. E. Moore, M.-C. Fok, and H. J. Singer (2004), Response of neutral atom emissions in the low- and high-latitude magnetosheath direction to the magnetopause motion under extreme solar wind conditions, *J. Geophys. Res.*, *109*, A04208, doi:10.1029/2003JA010147.
- Taguchi, S., S.-H. Chen, M. R. Collier, T. E. Moore, M.-C. Fok, K. Hosokawa, and A. Nakao (2005), Monitoring the high-altitude cusp with the low energy neutral atom imager: Simultaneous observations from IMAGE and Polar, *J. Geophys. Res.*, *110*, A12204, doi:10.1029/2005JA011075.
- Tsyganenko, N. A., and D. P. Stern (1996), Modeling the global magnetic field of the large-scale Birkeland current systems, *J. Geophys. Res.*, *101*, 27,187–27,198.
-
- M. R. Collier and T. E. Moore, NASA Goddard Space Flight Center, Greenbelt, MD 20771, USA.
- H. U. Frey and S. B. Mende, Space Science Laboratory, University of California, 7 Gauss Way, Berkeley, CA 94720–7450, USA.
- K. Hosokawa and S. Taguchi, Department of Information and Communication Engineering, University of Electro-Communications, Tokyo 182-8585, Japan.
- S. Suzuki, Sugadaira Space Radio Observatory, University of Electro-Communications, Tokyo 182-8585, Japan. (shin.s@ice.ucc.ac.jp)